Journal of the European Ceramic Society 22 (2002) 1917–1926

www.elsevier.com/locate/jeurceramsoc

Plastic forming and microstructural development of α-alumina ceramics from highly compacted green bodies using extrusion

C. Kaya*, E.G. Butler

Interdisciplinary Research Centre (IRC) in Materials Processing, The University of Birmingham, Edgbaston, Birmingham B15 2TT, UK

Received 8 May 2001; received in revised form 15 November 2001; accepted 8 December 2001

Abstract

High density (>99% TD) and microstructurally controlled α-alumina ceramics were produced from seeded nano-size boehmite (γ-AlOOH) sols with a very fine crystallite size (2–3 nm). A totally wet processing technique comprising vacuum filtering and pressure filtration (PF) was applied in order to increase the solids-loading of the sol and hence form an extrudable paste suitable for plastic forming using extrusion. High packing densities (>68% TD in the green state) are achieved by PF starting from the slurry state resulting in the formation of a consolidated paste which is further consolidated by extrusion. This combined processing technique was successfully applied, in an attempt to reduce the γ-Al_2O_3 formation temperature, and hence lower the θ- to α-Al_2O_3 transition temperature. The microstructure of dense α-Al_2O_3 bodies derived from seeded boehmite sol contains very fine (250 nm) alumina grains after sintering at 1200 °C for 2 h. Although the DTA evidence points to a θ- to α-Al_2O_3 transition temperature of 1208 °C for a seeded (with 30 nm TiO_2) sample, X-ray analysis indicates that a seeded, pressure filtrated and extruded sample is transformed to α-Al_2O_3 phase after sintering at 1100 °C for 2 h.

Keywords: Al_2O_3; AlOOH; Extrusion; Microstructure; Pressure filtration; Seeding; Sol-gel processes

1. Introduction

For the preparation of high-density α-alumina ceramics using colloidal processing, and to attain a uniform microstructure and favorable thermomechanical properties, some critical requirements, such as purity, particle/agglomerate size and green density need to be carefully controlled in order to achieve desirable properties.[1,2] It has been shown that α-alumina ceramics with high sintered densities can only be produced at lower sintering temperatures (<1200 °C), if the starting α-alumina powders are finer than 30 nm.[3] Experimental studies to date prove that it is very difficult and expensive to control the above mentioned parameters, thus, many workers have concentrated on preparing high quality α-alumina ceramics using very fine (10–100 nm) and sinter-active powders in the hydrous state, such as boehmite.[4–16] The high surface area to volume ratio of a ceramic sol makes the material usually highly sinter-active, thus sintering temperatures can be lowered by several hundred degrees as a result of enhanced sintering rates. Pseudo-boehmite (γ-AlOOH) is the most commonly used precursor for preparing high-purity and high-strength monolithic α-alumina ceramics by sol-gel technology. Microstructurally controlled boehmite-derived high-purity α-alumina ceramics with enhanced mechanical and thermomechanical stability, chemical inertness, optical and electrical properties, are widely used in a variety of applications, such as substrates for electronic circuits, abrasive grains, high temperature refractory materials, fibers and thin films. Boehmite is also a crucial precursor for preparing γ-Al_2O_3 which is used as a high-temperature catalyst support and as a membrane due to its high surface area and mesoporous properties.[17]

During thermal treatment, boehmite undergoes a series of metastable transition alumina phases, including γ-, δ-, θ-Al_2O_3, finally forming thermodynamically stable α-Al_2O_3.[3–7,9–16] The first transformation from pseudo-boehmite (γ-AlOOH) to γ-Al_2O_3 , where the orthorhombic crystal structure changes to the metastable spinel structure, occurs at about 500–550 °C, associated with density changes from 3.01 to 3.2 g/cm^3, as a result of the dehydration of boehmite. During the transformation of crystal structure from monoclinic phase (θ-Al_2O_3,

* Corresponding author. Tel.: +44-121-414-3537; fax: +44-121-414-3441.

E-mail address: c.kaya@bham.ac.uk (C. Kaya).

0955-2219/02/$ - see front matter
PII: S0955-2219(01)00523-4

$d = 3.56$ g/cm^3) to hexagonal phase (α-Al_2O_3, $d = 3.986$ g/cm^3), a volume reduction of about 10% occurs because of the higher density of the α phase. As a result of density and molecular weight changes, the total volumetric shrinkage of boehmite caused by the transformation plus densification until the stable α-Al_2O_3 is formed may vary from about 30 to 40% depending upon the starting boehmite crystallite size. Without seeding, boehmite sol requires very high sintering temperatures (>1600 °C) for complete densification because of the large and extensive pore network that develops during the reconstructive transformation of boehmite to the final stable phase of α-Al_2O_3. Seeding the boehmite sol with crystallographically suitable modifiers reduces the crystallization temperature for the final α-Al_2O_3 phase, accelerates the transformation kinetics, reduces the sintering temperature and enhances densification[9–13] due to operation of nucleation and growth mechanisms. However, the seeding is a very complex process and some critical parameters, such as concentration, size, crystallinity and purity of the seeds, and also heating atmosphere must be controlled to achieve high-density alumina components with controlled microstructures.

The main objective of the present work is to develop and control the α-alumina microstructure obtained from boehmite sols seeded with ultra-fine (30 nm) particles using the concept of high-density-particle-packing, constrained densification, and reduction in the formation temperature of α-alumina. For this aim, a totally wet processing route was employed including pressure filtration, resulting in the formation of a high solids-loading extrudable paste with high green density followed by extrusion which provides further consolidation and preferential grain alignment. It had been shown that almost full density (99.4% T.D) α-alumina ceramics with a very fine microstructure can be produced at low sintering temperatures if the green density of the compact is optimised by improved particle packing during the consolidation process.

2. Experimental work

2.1. Pseudo-boehmite (γ-AlOOH) and seeding

Commercially available pseudo-boehmite (γ-AlOOH) sol (Remal A20, Remet corp., USA) was used as the alumina source. The sol has average particle size and solids-loading of 40 nm and 20 wt.%, respectively. As received sol is stable at a pH value of 3–4. Our TEM observations have showed that the individual boehmite particles are lath shaped and that there is no flocculation within the sol (see Fig. 1). The as received boehmite sol was seeded with 2 wt.% of the total mass using three different seeding powders, as detailed in Table 1. To seed the boehmite sol, each of the seeding powders was

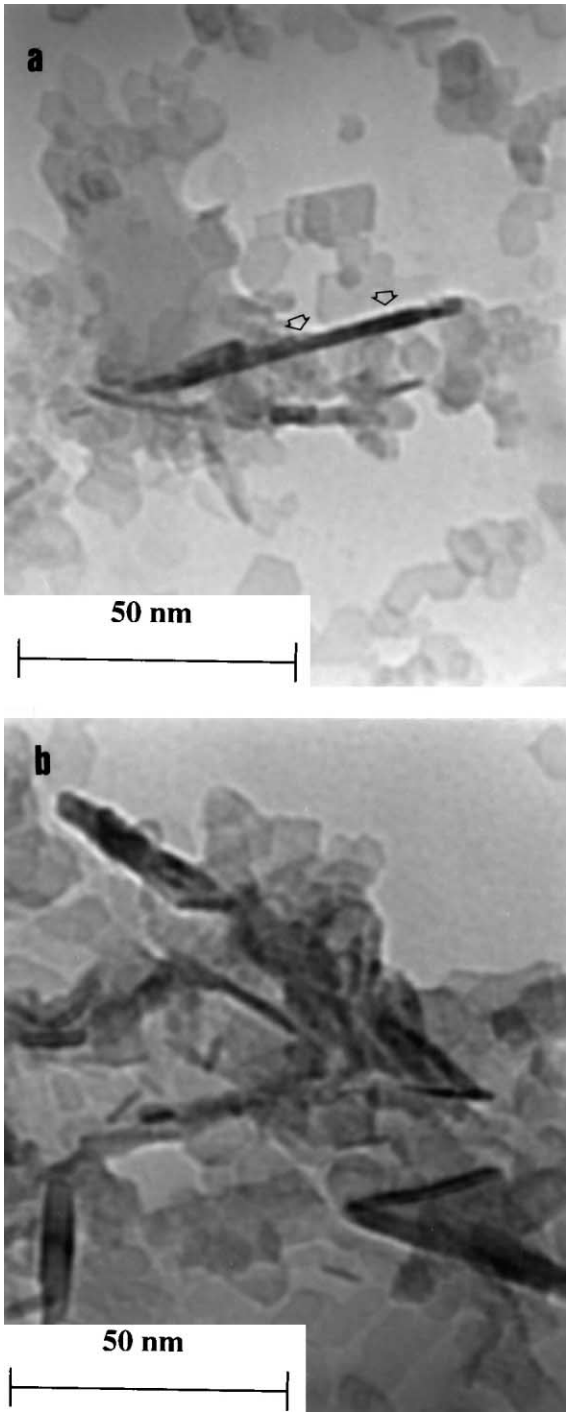

Fig. 1. Bright-field TEM micrographs of (a) the as received boehmite and (b) seeded boehmite sol microstructures.

first dispersed in distilled water and then added into boehmite sol. 1 wt.% glycerol was also added in order to minimise the surface roughness of the extruded rods during extrusion. The seeded sol was first stirred magnetically for 10 h and then ultrasonic agitation was employed at 15 kHz for 3 h for further dispersion of any particle agglomerates which might be present. The final sol composition i.e. boehmite + 2 wt.% seeding powder + 1

Table 1
The average particle size of the seeding powders and their effect on the boehmite decomposition and θ- to α-alumina transition temperature

Seeding powder	Average particle size (nm)	DTA boehmite decomposition temperature (°C)	DTA θ- to α-Al_2O_3 transition temperature (°C)
α-Al_2O_3[a]	200	450	1225
α-Al_2O_3[b]	30	450	1210
TiO_2[c]	30	440	1208

[a] Taimicron TM-DAR, Taimei CHBS Chemicals, Japan.
[b] BDH Chemicals, UK (high purity polishing powder).
[c] Degussa, Ltd., Germany.

wt. % glycerol was ball-mixed for 2 days using high purity TZP balls. Before and after ball-milling, the TZP balls were weighted to ensure that there was no contamination resulting from the milling media. The mixed seeded sol was then vacuum filtered in order to obtain a gel structure. The resulting soft white gel was compacted using pressure filtration apparatus to squeeze out the excess water and obtain an extrudable paste as explained in the following section (detailed information about the application of this technique can be found elsewhere.[18] The sol/gel paste was then extruded using a laboratory scale extrusion apparatus with an extrusion reduction ratio of 10:1. The consolidated green samples, i.e. pressure filtrated and extruded, were first kept in a humidity controlled chamber (from 80 to 55% relative humidity) for 1 day to allow the residual water to remove slowly from the green body, thus preventing the formation of any internal cracks. This was followed by 1 day drying in normal air. The dried green body compacts were pressureless sintered at different temperatures for 2 h in air using a 3 °C/min heating and cooling rate.

2.2. Paste formation by pressure filtration

The pressure filtration (PF) technique, which involves the mechanical application of pressure to a slurry in order to force the suspension through a filter assembly, was employed for the formation of alumina green bodies. This colloidal wet forming method eliminates the use of some intermediate processing steps, such as drying and milling of the sol derived materials. In these experiments, a constant load of 100 kN was applied cyclicly using a constant ram displacement rate of 0.5 mm/min. After reaching the maximum load, the ram displacement was held for 10 min. and then the load was removed using the same rate. Finally, compacted extrudible paste was removed and extruded immediately.

2.3. Grain size measurements by 'linear intercept' technique

In this method, a random line is drawn on a micrograph and the number of grain boundaries intercepting the line are counted. In order to obtain the average grain size of the alumina phase, a good quality micrograph showing the grains of the alumina phase was obtained by Field Emission Gun (FEG) SEM or TEM. A transparent sheet containing one or more test lines of known length was fixed in place over the micrograph, then the number of intercepts between the test lines and grain boundaries were counted. The average grain size of alumina were calculated using the equations published in the literature.[19,20]

2.4. Phase evaluation by X-ray diffraction (XRD)

Powder and sintered samples were calcined at different temperatures and then analysed using X-rays (CuK radiation and nickel filter to remove the Cu K_β peak, Philips X'Pert, Germany), operated at 40 keV and 30 mA. The diffractometer scanned from 5 to 80° with a scan step of 0.02° 2θ and a count time of 2 s per step. Phase identification was carried out using a computer controlled X-ray diffractometer and the obtained peaks were compared with the d-spacing for standard phase compositions listed in the JCPDS-ICDD archive.

2.5. Differential thermal analysis (DTA) and thermal gravimetric analysis (TGA)

Powder samples were subjected to differential thermal analysis (DTA) and thermal gravimetric analysis (TGA) under static air atmosphere using a Stanton Redcroft STA781 simultaneous DTA/TGA apparatus in order to determine the phase transformation temperatures and related mass loss. High purity α-alumina was used as a reference material. Phase transformation temperatures and mass loss were measured by a thermocouple and an electronic hang-down balance, respectively. These data were collected and analysed using a computer linked to the equipment. All experiments were carried out using a fixed sample mass (15–20 mg$\pm$0.01 mg) and heating rate (10 °C/min).

3. Results and discussions

3.1. Particle size and seeding

Fig. 1 shows Bright-Field TEM micrographs of the (a) un-seeded and (b) seeded with 30 nm α-alumina, boehmite particles within the sol, with an average particle size of 40 nm. Both micrographs show that boehmite particles are lath shaped and well distributed. There are no heteroflocculated long boehmite chains which is the indication of a kinetically stable sol microstructure. Although the dominant boehmite particle shape is lath like, it should also be noted that the as received boehmite sol, shown in Fig. 1(a) contains some

ultra-fine (5–10 nm) hexagonal boehmite species, as well. This is considered to be effective in achieving high packing densities after the first consolidation process of pressure filtration.

The average particle size of the seeding powders and their effect on the decomposition and transformation temperature of boehmite to α-alumina is given in Table 1, as determined by DTA measurements. Seeding the boehmite sols with ultra-fine (30 nm) TiO_2 and α-Al_2O_3 seeds resulted in the formation of α-Al_2O_3 at almost simultaneous transformation temperatures of 1208 and 1210 °C, respectively. However, as the particle size of the seeding powder is increased to 200 nm, the transformation temperature of boehmite to α-Al_2O_3 was observed to be 1225 °C. The DTA and TG traces (heating rate 10 °C/min) of TiO_2 (30 nm) and α-Al_2O_3 (200 nm) seeded boehmite are shown in Figs. 2 and 3, respectively. Both seeded boehmites exhibit significant weight loss at 100 and 450 °C, corresponding to the desorption (or removal) of free water from the boehmite particle surface and dehydration of OH groups during the phase transition from γ-AlOOH to γ-Al_2O_3. As shown in Fig. 2(a), the TiO_2 seeded boehmite showed a total weight loss of 43.5% (starting weight: 16.3 mg and finishing weight: 9.2 mg) and decomposes at 440 °C with the presence of a sharp endothermic peak in the DTA trace. The DTA curve showed a major exothermic peak at 1208 °C, as shown in detail in Fig. 2(b), confirming the θ- to α-alumina transition taking place at this temperature. The differences in DTA and TG traces of TiO_2 (30 nm) and α-Al_2O_3 (200 nm) seeded boehmite are the total weight loss and the transition temperature, as the graph of α-Al_2O_3 (200 nm) seeded boehmite is shown in Fig. 3. The decomposition temperature is 450 °C and the total weight loss is 48% (starting mass is 16.3 mg and the finishing mass is 8.4 mg) for α-Al_2O_3 (200 nm) seeded boehmite, as shown in Fig. 3(a). The transition temperature is determined to be 1225 °C [see Fig. 3(b)] which is higher than that ones obtained from TiO_2 (1208 °C) and finer (30 nm) α-Al_2O_3 seeded boehmite (1210 °C).

From the Figs. 2 and 3, it is clear that both ultra-fine (30 nm) TiO_2 and α-Al_2O_3 (200 nm) seeding materials lower the decomposition temperature by at least 50 °C and the θ- to α-alumina transition temperature by 15 °C. There have been many experimental studies on the effects of the seeding materials on the phase transformation behaviour of boehmite.[3–16] Normally different micron-size seeding materials have been used, and as far as the present work is concerned, such ultra-fine seeds (30 nm) have not previously been reported. Although DTA and TG analysis indicated θ- to α-alumina transition temperatures of 1208, 1210 and 1225 °C for TiO_2, α-Al_2O_3 (30 nm) and α-Al_2O_3 (200 nm) seeding materials, respectively, additional phase analysis was carried out on the pressure filtrated and extruded compacts in order to identify the effect of the consolidation processes on the final phase formation of boehmite as a function of sintering temperature. The results are shown in Table 2. The consolidated seeded compacts transformed to α-Al_2O_3 at a temperature as low as 1100 °C for 2 h. Previously, it has been shown that α-Al_2O_3 ceramics can be produced from seeded boehmite at sintering temperatures as low as 1025 °C, provided the state of boehmite dispersion during mixing is optimised to a more uniform sol/gel microstructure.[3] In the present work, since no pre-treatment was applied, some different mechanism could be responsible for the early formation of α-Al_2O_3. The as received boehmite and seeded boehmite sol microstructures shown in Fig. 1 show that the lath shape boehmite particles are very well dispersed and there is no evidence of the presence of any large agglomerates. This kind of uniform sol microstructure should improve sinterability and reduce the transition temperature. Also, it has been shown recently that the formation temperature of γ-Al_2O_3 from boehmite and the phase transition temperature from θ-Al_2O_3 to α-Al_2O_3 increases with increasing boehmites crystallite size. γ-Al_2O_3 formation mechanism is related to the crystallite size of boehmite and is nucleation controlled in large crystallites, phase-boundary controlled in medium-sized crystallites, and diffusion controlled in small crystallites.[21,22] Boehmite has an orthorombic unit cell with the axes: $a = 2.861$, $b = 3.696$, and $c = 12.233$ Å[23] and the crystal structure consists of chains of AlO_6 octahedra giving double molecules, as shown:[23]

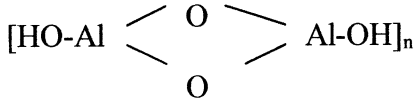

Al–O octahedral double layers which are connected by hydrogen bonds are parallel and form layers with OH groups outside.[22,23] During the transformation of boehmite to γ-Al_2O_3, dehydration takes place. As the crystallite size is increased, dehydration paths within the boehmite structure become longer and the interlayer spacing narrow.[22] Dehydration, therefore, progresses slowly and suppresses the conversion of boehmite to γ-Al_2O_3, resulting in an increase in the formation

Table 2
Alumina phases[a] within the pressure filtrated and extruded compacts as a function of sintering temperature (°C) for a constant holding time of 2 h, as determined by XRD

Materials	Sintering temperature (°C)		
	1075	1100	1125
Un-seeded boehmite	δ + θ + α	θ + α	θ + α
α-Al_2O_3 (30 nm) seeded	θ + α	α	α
α-Al_2O_3 (200nm) seeded	θ + α	θ + α	α
TiO_2 seeded	θ + α	α	α

[a] α, α-Al_2O_3; δ, δ-Al_2O_3; θ, θ-Al_2O_3.

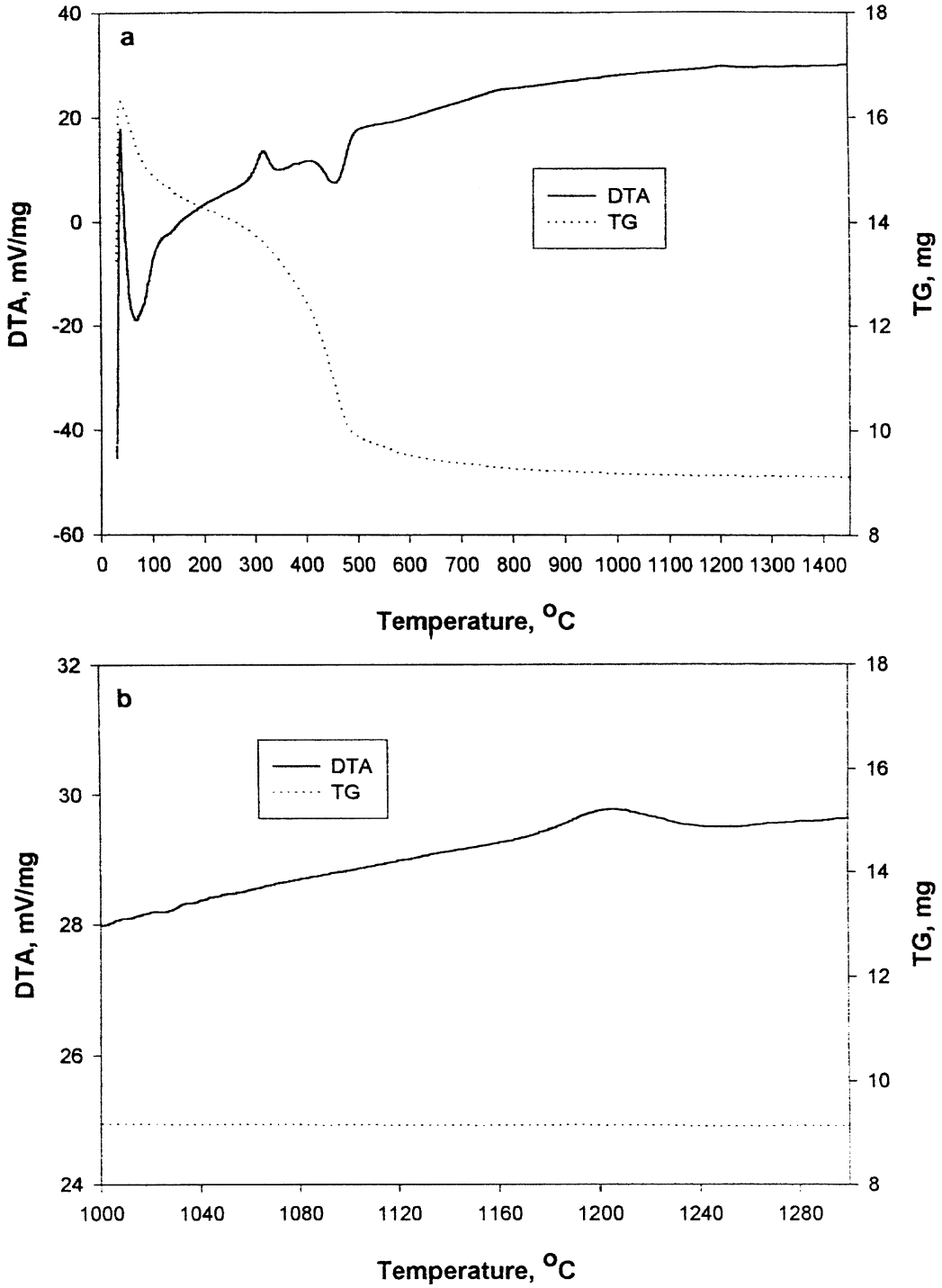

Fig. 2. (a) DTA and TGA traces for TiO_2 (30 nm) seeded boehmite and (b) the detail section of 1000–1300 °C in order to clarify the transition temperature.

temperature of the γ-alumina phase. On the other hand, there is also a close relation between the crystallinity of boehmite and the transformation temperature of γ-Al_2O_3. The higher amount of residual OH groups in γ-Al_2O_3 decreases the crystallinity of boehmite, and the reconstruction of the cubic close-packed to a hexagonal oxygen sublattice during the transition from θ- to α-Al_2O_3 takes place at a lower temperature in a transition alumina of lower crystallinity.[21] The as received pseudo-boehmite used in this work has a very small crystallite size (2–3 nm), thus accelerating γ-AlOOH dehydration and γ-Al_2O_3 formation and resulting in an early transition from θ- to α-Al_2O_3 at low temperatures (as low as 1100 °C). The low crystallinity of boehmite due to high OH content is also evident from the TG traces, shown in Figs. 2 and 3.

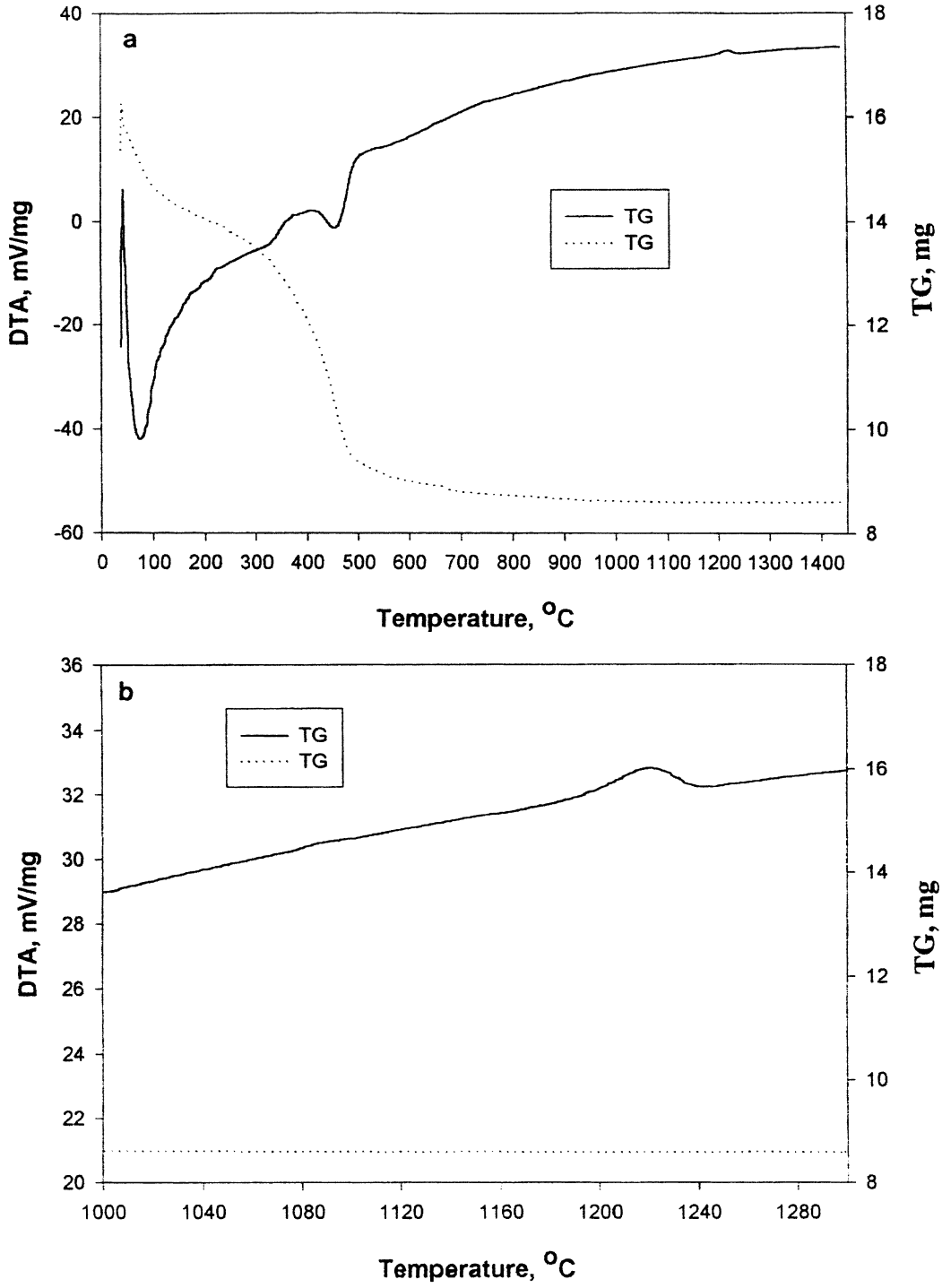

Fig. 3. (a) DTA and TGA traces for α-Al_2O_3 (30 nm) seeded boehmite and (b) the detail section of 1000–1300 °C in order to clarify the transition temperature.

It has already been proven that after complete transition from θ- to α-Al_2O_3 (the crystal structure changes from monoclinic to hexagonal), two typical morphologies of transformed α-Al_2O_3 could be seen.[7,11] The first one known as "discrete" forms at about 1000 °C and contains very fine α grains (< 500 nm), whilst the second type of morphology known as "vermicular", is formed as a result of finger growth of α-Al_2O_3 grains into the θ-Al_2O_3 matrix at 1150–1200 °C and results in the formation of porous channels during transformation. The high resolution scanning electron micrograph (Fig. 4) shows that the transformed α-Al_2O_3 microstructure contains very fine (210 nm) equiaxed α grains after sintering at 1100 °C for 2 h. The formation of a vermicular

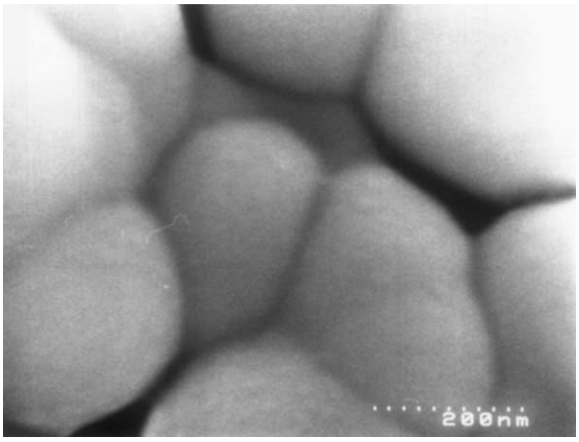

Fig. 4. Scanning electron micrograph of α-Al_2O_3 matrix obtained from α-Al_2O_3 (30 nm) seeded boehmite after sintering at 1100 °C for 2 h. Note the presence of equiaxed alumina grains with no porosity.

morphology, which is difficult to sinter, is avoided by using ultrafine (30 nm) α-Al_2O_3 or TiO_2 seeds. It is also believed that the ultrafine α-Al_2O_3 or TiO_2 seeds provide the nucleation sites to lower the activation energy and phase transformation temperature.[3] In the case of α-Al_2O_3 seeding, as the phase transformation proceeds, initially α-Al_2O_3 nuclei appear at certain sites in the θ phase and then α-Al_2O_3 nuclei start to grow into the surrounding θ phase. As the α-Al_2O_3 grains grow, the interface between the α-Al_2O_3 and the θ-Al_2O_3 matrix migrates into θ-Al_2O_3 matrix (so called "interface control mechanism"). This finding is in good agreement with the published data.[4,15] A bright-field TEM micrograph prepared from a sample sintered at 950 °C for 2 h, clearly shows that an α-Al_2O_3 grain has begun to grow into the surrounding metastable θ-Al_2O_3 matrix, as shown in Fig. 5. It is also noted from Fig. 5 that the θ phase which surrounds the growing α-Al_2O_3 matrix has

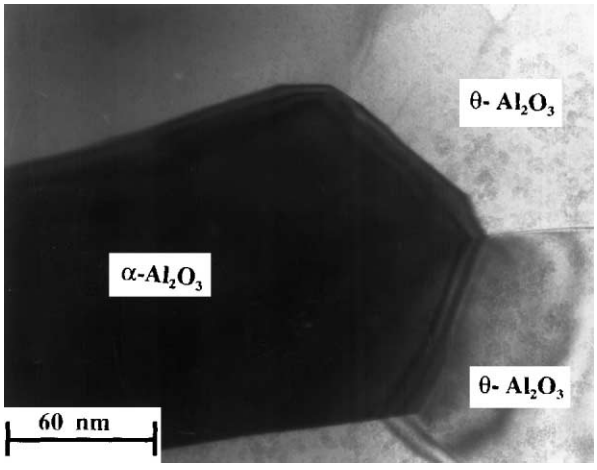

Fig. 5. Bright-field TEM micrograph, showing the growing direction of an α-Al_2O_3 grain into θ-alumina matrix after sintering at 950 °C for 2 h. Also note that the porous structure of metastable θ-alumina matrix which surrounds the α-alumina phase.

a porous nature. From the results presented in Figs. 4 and 5, it is concluded that during the early transition from θ- to α-Al_2O_3, the oxygen atoms diffuse from the θ matrix across the boundary during transformation to α phase. The lattice diffusion of oxygen in alumina is probably the controlling mechanism of the θ- to α-Al_2O_3 transformation.[24] The transformation proceeds through the growth of seeds, thus the main transformation mechanism is the structural rearrangement by the diffusion of oxygen in the alumina lattice.

3.2. Pressure filtration and extrusion

The effects of the combined consolidation processes, i.e. pressure filtration and extrusion on the green and sintered densities of the seeded compacts, are shown in Table 3. The use of pressure filtration is able to increase the green density up to 68.5% TD, and this value is further increased to 71.4% TD using extrusion. Table 3 shows also that regardless of the seeding materials used, similar green densities are obtained from all the seeded compacts. These green densities are significantly high, thus it is believed that densification is enhanced by decreasing pore size and narrowing its distribution in the green compact using two-step consolidation process,[25] leading to an increase in sintering density and decrease in sintering temperature of the transition alumina phases. Resulted green body with higher density (71.4% TD) increases the contact area of neighbouring particles and reduces the volume of micro-pores, enhances the densification process and lowers the sintering temperature. The main driving force in ceramic sintering is the high surface free energy of particles. The smaller the particle size, the higher the surface free energy, the easier of surface atom diffusion between neighbouring particles, and the lower sintering temperature.[26] The combined consolidation technique used in this work provides high green-body-density, and correspondingly the total contact surface area is increased, thus this enhances the surface diffusion due to shorter diffusion distances. It is concluded that during pressure filtration, lath shape boehmite particles are easily deformed and compacted. It is also noted that the boehmite sol used contains the right combination of

Table 3
Green and sintered densities (% TD) of the seeded boehmite dependence on the consolidation process (sintered densities were measured on the samples sintered at 1300 °C for 2 h)

Seeding material	Green density (% TD)[a]		Sintered density (% TD)
	PF	PF + Ext.	
α-Al_2O_3 (200 nm)	68.1	70.4	98.3
α-Al_2O_3 (30 nm)	68.5	71.4	99.4
TiO_2	68.4	71.2	99.1

[a] PF, pressure filtration; Ext, extrusion.

particles with different sizes, as shown in Fig. 1, thus the combined effect of pressure and particle size resulting in high green densities which enhance densification and lower the temperature required for full density.[27] A 2-day milling was applied during the seeded sol preparation, thus, it is believed that increasing the milling time of these ultrafine powders also reduces the the crystallization temperature and enhances densification.

3.3. Sintering

Grain size dependence of the pressure filtrated and extruded boehmite derived alumina on the seeding powder as a function of sintering temperature is given in Table 4. TiO_2 seeding (30 nm) provides the finest grain size at all sintering temperatures whilst coarse seed material (200 nm) results in the coarser grain size (the diffusion rate of TiO_2 into alumina matrix is very high, thus it also reduces the formation temperature of α-Al_2O_3, as explained earlier). The alumina matrix contains submicron grains at sintering temperatures up to 1300 °C and then a significant increase in grain size up to 1400 °C is seen. However, compacts sintered at 1500 °C show the indication of abnormal grain growth for all seeding materials. The average grain size of TiO_2 seeded alumina is 240 nm after sintering at 1100 °C for 2 h and it increases to 3.5 μm at 1500 °C. Seeding boehmite with α-Al_2O_3 (30 nm) results in the formation of alumina grains with an average grain size of 250 nm at 1100 °C and it icreases to 5.1 μm when it is sintered at 1500 °C for 2 h. In order to clarify the effects of different seeding powders on the microstructure of boehmite derived alumina in terms of grain shape, pore size and distribution, scanning electron micrographs of α-Al_2O_3 (30 nm) and TiO_2 (30 nm) seeded microstructures, are shown in Figs. 6 and 7, respectively. Alumina matrix microstructure derived from α-Al_2O_3 (30 nm) seeded boehmite contains very fine grains after sintering at 1200 °C for 2h, as shown in Fig. 6(a) with the presence of no intra- or inter-granular porosity. As the sintering temperature is increased to 1400 or 1500 °C for the same sintering time of 2 h, α-Al_2O_3 grains start to grow, as shown in Fig. 6(b) and (c), respectively. Samples produced from α-Al_2O_3 seeded boehmite contains only inter-granular pores after sintering at 1400 °C whilst samples sintered at 1500 °C show the evidence of formation of intra-granular porosity, as abnormal grain growth takes place at this temperature, as shown in Fig. 6 (b) and (c), respectively. This suggests that α-

Table 4
Grain size (μm) dependence of the pressure filtrated and extruded boehmite derived alumina on the seeding powder as a function of sintering temperature for a constant holding time of 2 h

Seeding powder	Sintering temperature (°C)				
	1100	1200	1300	1400	1500
α-Al_2O_3 (200 nm)	0.3	0.33	0.47	3.8	7.4
α-Al_2O_3 (30 nm)	0.25	0.27	0.34	2.4	5.1
TiO_2	0.24	0.25	0.33	2.1	3.5

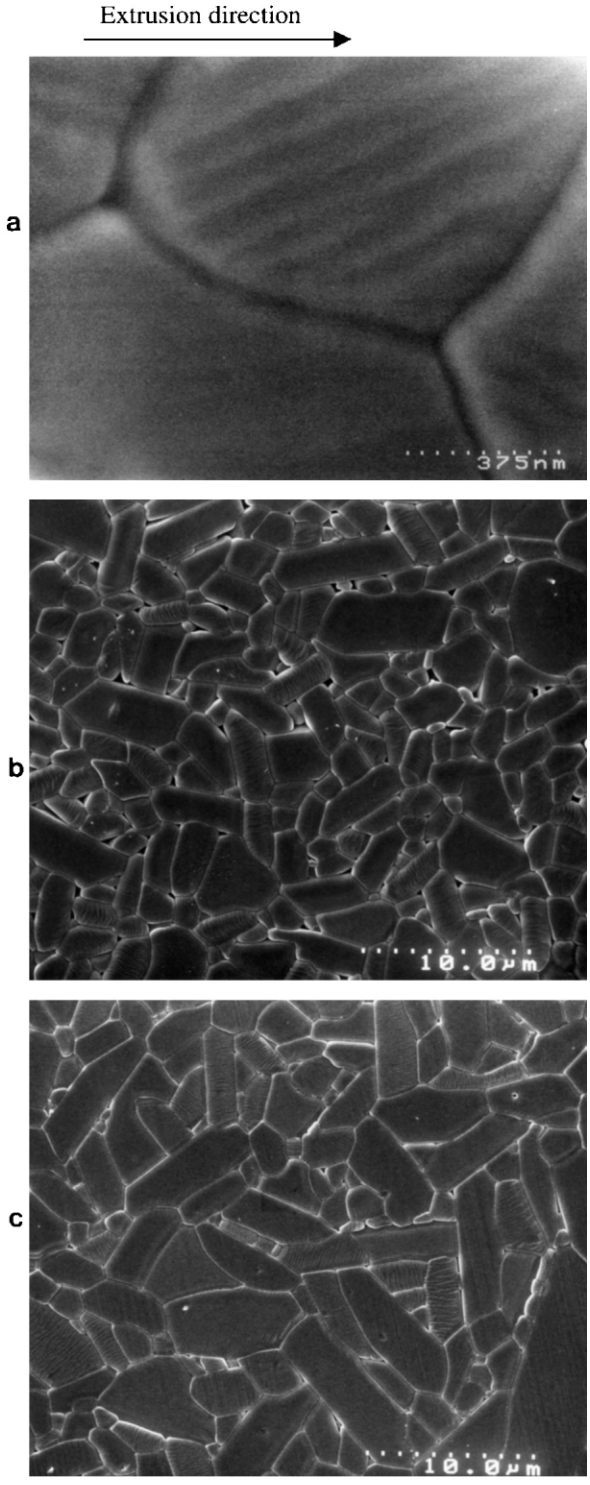

Fig. 6. Scanning electron micrographs of α-Al_2O_3 matrix obtained from α-Al_2O_3 (30 nm) seeded boehmite after sintering at (a) 1200 °C, (b) 1400 °C, and (c) 1500 °C for 2 h. Note the presence of significant α-Al_2O_3 grain alignment parallel to the extrusion direction after sintering at high temperature (b) and (c).

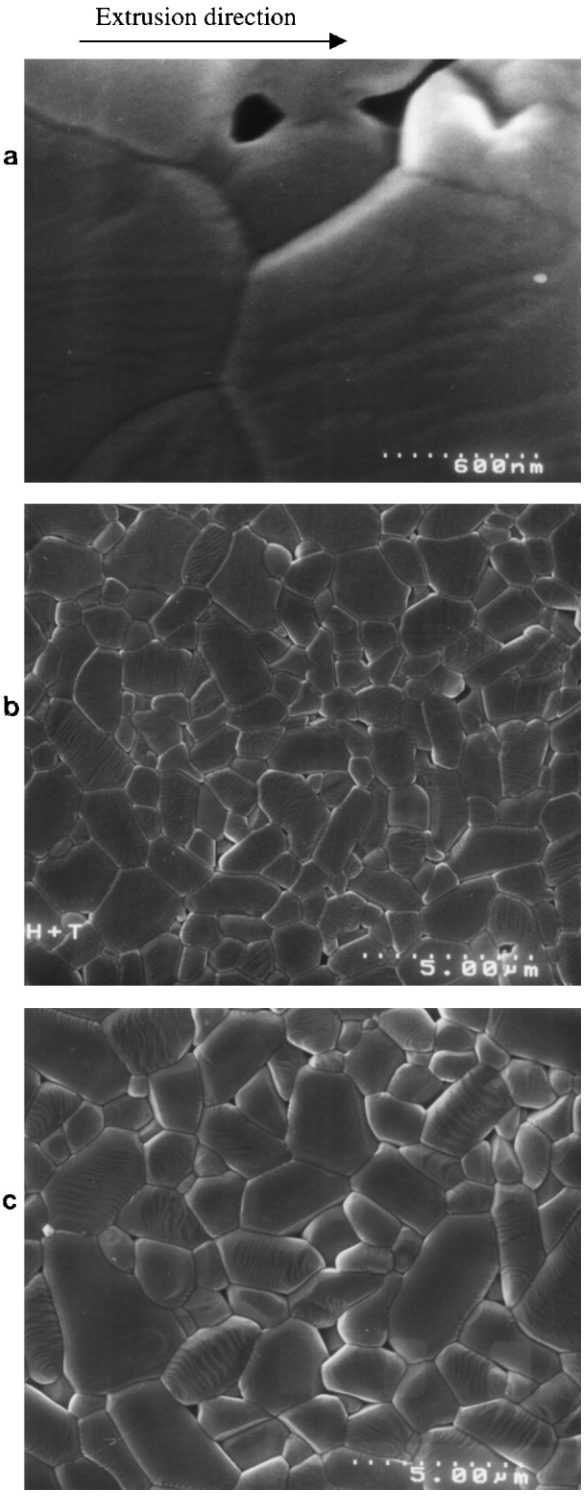

Fig. 7. Scanning electron micrographs of α-Al_2O_3 matrix obtained from TiO_2 (30 nm) seeded boehmite after sintering at (a) 1200 °C, (b) 1400 °C, and (c) 1500 °C for 2 h. Note the absence of any elongated grains at high temperatures (b) and (c).

Al_2O_3 grains grow and eliminate the sub-micron size (0.4 μm) inter-granular pores during the diffusion process, leading to the formation of elongated alumina grains, especially, as shown in Fig. 6(c). However, alumina microstructure obtained from TiO_2 seeded boehmite shows a significant difference in grain and porosity morphology, as shown in Fig. 7. Sample sintered at 1200 °C for 2 h contains fine equiaxed α-Al_2O_3 grains (250 nm) with the presence of inter-granular porosity (0.2 μm), as shown in Fig. 7(a). Although abnormal grain growth occurred on samples sintered at 1400 or 1500 °C, there is no intra-granular pore formation, and α-Al_2O_3 grains are equiaxed, as shown in Fig. 7(b) and (c), respectively. Figs. 6 and 7 also indicate that some of the grains grow parallel to the extrusion direction but majority of the grains aligned with a 30° angle to the extrusion direction. This is the dominant matrix morphology, particularly for alumina obtained from α-Al_2O_3 seeded boehmite, as shown in Fig. 6.

One of the significant results of θ- to α-Al_2O_3 transformation is the associated grain growth leading to the changes in α-Al_2O_3 grain size and morphology. Although densification during pressureless sintering of θ alumina is known to be slow due to vermicular structure developed from the transformation, the alumina microstructure produced in this study, depending on the seeds, shows equiaxed grains (at sintering temperatures up to 1300 °C) or elongated grains (at sintering temperatures up to 1500 °C), as shown in Figs. 4, 6 and 7. From these results, it can be concluded that the PF and extrusion lead to equiaxed morphology after transformation of θ to α alumina. This grain morphology also helps to accelerate densification rate. From Tables 3 and 4 and Figs. 6 and 7, it appears that the ideal sintering temperature for the pseudo-boehmite used in this work, is about 1200–1300 °C where abnormal grain growth does not occur. This low sintering temperature resulted from the high green density is also helpful because the grain boundary mobility is lower at these temperatures and therefore excessive grain growth is avoided,[28] as shown in Figs. 4, 6 and 7.

4. Conclusion

Pseudo-boehmite (γ-AlOOH) with a very small crystallite size (2–3 nm) can be seeded with ultrafine (30 nm) α-Al_2O_3/TiO_2 and coarser (200 nm) α-Al_2O_3 powders in order to lower the DTA θ- to α-Al_2O_3 transition temperatures. Seeding boehmite with ultrafine powders (30 nm) reduces the transformation temperature to 1208–1210 °C whilst seeding boehmite with coarser powders (200 nm) results in the α-Al_2O_3 formation at 1225 °C. However, pressure filtrated and extruded seeded boehmite derived alumina matrix contains only α-Al_2O_3 phase after sintering at 1100 °C for 2 h, as determined by XRD, indicating the significant contribution of the compaction process on the transformation temperature. The following conditions are believed to be responsible for early formation of γ-Al_2O_3, leading to lower the θ-

to α-Al_2O_3 transition temperatures; homogeneous and agglomerate free starting sol microstructure and the use of ultrafine seeds combined with a two-step consolidation process (pressure filtration and extrusion) leading to high packing densities in the green state. Samples produced from boehmite seeded with ultrafine powders contain very fine α-Al_2O_3 grains (250 nm) after pressureless sintering at 1200 °C for 2 h. These microstructures are expected to provide good mechanical and thermomechanical properties.

Acknowledgements

This project is supported by the European Commission under the contract number BRITE-EURAM, BRPR-CT 97–0609.

References

1. Yen, T. S. and Sacks, M. D., Low-temperature sintering of aluminum oxide. *J. Am. Ceram. Soc.*, 1988, **7**, 841–844.
2. Rajendran, S., Production of ultrafine alpha-alumina powders and fabrication of fine-grained strong ceramics. *J. Mater. Sci.*, 1994, **29**, 5664–5672.
3. Messing, G. L. and Kumagai, M., Low-temperature sintering of α-Al_2O_3-seeded boehmite gel. *Amer. Ceram. Soc. Bull.*, 1994, **73**, 88–93.
4. Kumagai, M. and Messing, G. L., Enhanced densification of boehmite-sol-gels by α-alumina seeding. *J. Am. Ceram. Soc.*, 1984, **67**, C230–C231.
5. McArdle, J. L. and Messing, G. L., Transformation, microstructure development, and densification of α-Fe_2O_3 seeded boehmite derived alumina. *J. Am. Ceram. Soc.*, 1993, **76**, 214–222.
6. McArdle, J. L., Messing, G. L., Tietz, L. A. and Carter, C. B., Solid-phase epitaxy of boehmite-derived α-alumina on hematite seeds crystals. *J. Am. Ceram. Soc.*, 1989, **72**, 864–867.
7. Badkar, P. A. and Bailey, J. E., The mechanism of simultaneous sintering and phase transformation in alumina. *J. Mater. Sci.*, 1976, **11**, 1794–1806.
8. Kaya, C., Boccaccini, A. R. and Chawla, K. K., Fabrication and characterisation of Ni-coated carbon fibre-reinforced alumina ceramic matrix composites using electrophoretic deposition. *Acta Mater.*, 2001, **49**, 1189–1197.
9. Shelleman, R. A., Messing, G. L. and Kumagai, M., Alpha-alumina transformation in seeded boehmite gels. *J. Non-Crytal. Solids*, 1986, **82**, 277–285.
10. Dynys, F. D., Lungberg, M. and Halloran, J. W., Microstructural transformation in alumina gels. *Mater. Res. Soc. Symp. Proc.*, 1984, **32**, 321–326.
11. Dynys, F. D. and Halloran, J. W., Alpha-alumina formation in gels. In *Ultrastructure processing of ceramics, glasses, and composites*, ed. L. L. Hench and D. R. Ultrich. Wiley, New York, 1984.
12. Dynys, F. D. and Halloran, J. W., Alpha-alumina formation in Alum-derived gamma-alumina. *J. Am. Ceram. Soc.*, 1982, **65**, 442–448.
13. Messing, G. L., Kumagai, M., Shelleman, R. A. and McArdle, J. L., Seeded transformation for microstructural control in ceramics. In *Science of ceramic chemical processing*, ed. L. L. Hench and D. R. Ulrich. Wiley, New York, USA, 1986, pp. 259–271.
14. Pach, L., Roy, R. and Komarneni, S., Nucleation of alpha-alumina in boehmite gel. *J. Mater. Res.*, 1990, **5**, 278–285.
15. Kumagai, M. and Messing, G. L., Controlled transformation and sintering of a boehmite-sol-gel by α-alumina seeding. *J. Am. Ceram. Soc.*, 1085, **68**, 500–505.
16. McArdle, J. L. and Messing, G. L., Transformation and microstructure control in boehmite-derived alumina by ferric oxide seeding. *Adv. Ceram. Mater.*, 1988, **3**, 387–392.
17. Stiles, A. B., *Catalyst Supports and Supported Catalysts*. Butterworths, London, 1987.
18. Kaya, C. *Processing and Properties of Alumina Fibre-reinforced Mullite Ceramic Matrix Composites*. PhD thesis, The University of Birmingham, UK, June 1999.
19. Mendelson, M. I., Average grain size in polycrystalline ceramics. *J. Am. Ceram. Soc.*, 1969, **52**, 443–446.
20. Wurst, J. C. and Nelson, J. A., Linear intercept technique for measuring grain size in two-phase polycrystalline ceramics (discussion and notes). *J. Am. Ceram. Soc., 1972, 109*.
21. Tsukada, T., Segawa, H., Yasumori, A. and Okada, K., Crystallinity of boehmite and its effect on the phase transition temperature of alumina. *J. Mater. Chem.*, 1998, **9**, 549–553.
22. Tsuchida, T., Furuich, R. and Ishii, T., Kinetics of the dehydration of boehmites prepared under different hydrothermal conditions. *Thermochim. Acta*, 1980, **39**, 103–115.
23. Lippens, B. C. and De Boer, J. H., Study of phase transformations during calcination of aluminum hydroxides by selected area electron diffraction. *Acta Crystallogr.*, 1964, **17**, 1312–1321.
24. Kao, H. C. and Wei, W. C., Kinetics and microstructural evolution of heterogeneous transformation of θ-alumina to α-alumina. *J. Am. Ceram. Soc.*, 2000, **83**, 362–368.
25. Lin, F. T. J., De Jonghe, L. C. and Rahaman, M. N., Microstructure refinement of sintered alumina by a two-step sintering technique. *J. Am. Ceram. Soc.*, 1997, **80**, 2269–2277.
26. Kuang, X., Carotenuto, G. and Nicolais, L., A review of ceramic sintering and suggestions on reducing sintering temperatures. *Adv. Perfor. Mater.*, 1997, **4**, 257–274.
27. Nordahl, C. S. and Messing, G. L., Transformation and densification of nanocrystalline γ-alumina during sinter forging. *J. Am. Ceram. Soc.*, 1996, **79**, 3149–3154.
28. Mishra, R. S., Lesher, C. E. and Mukherjee, A. K., High-pressure sintering of nanocrystalline γ-Al_2O_3. *J. Am. Ceram. Soc.*, 1996, **79**, 2989–2992.